RSC Advances

PAPER

View Article Online
View Journal | View Issue

Cite this: *RSC Adv.*, 2023, **13**, 4932

A pH responsive and superporous biocomposite hydrogel of *Salvia spinosa* polysaccharide-*co*-methacrylic acid for intelligent drug delivery

Arshad Ali,[a] Muhammad Tahir Haseeb,[b] Muhammad Ajaz Hussain,[c]* Ume Ruqia Tulain,[b] Gulzar Muhammad,[d] Irfan Azhar,[e] Syed Zajif Hussain,[f] Irshad Hussain[f] and Naveed Ahmad[g]

Herein, a drug delivery system (SSH-*co*-MAA) based on the mucilage from seeds of *Salvia spinosa* (SSH; polymer) and methacrylic acid (MAA; monomer) is introduced for the controlled delivery of venlafaxine HCl using a sustainable chemical approach. The optimized conditions for the designing of the ideal formulation (M4) of SSH-*co*-MAA were found to be 2.5% (w/w) of SSH, 30.0% (w/w) of MAA, 0.4% (w/w) of both *N*,*N*′-methylene-bis-acrylamide (MBA; cross-linker) and potassium persulfate (KPS; initiator). The structure characterization of SSH-*co*-MAA by Fourier transform infrared and solid-state CP/MAS ^{13}C-NMR spectroscopy has confirmed the grafting of MAA onto SSH. The thermogravimetric analysis revealed that SSH-*co*-MAA is a stable entity before and after loading of the venlafaxine HCl-loaded SSH-*co*-MAA (VSSH-*co*-MAA). Scanning electron microscopy images of SSH-*co*-MAA after swelling then freeze drying showed the superporous nature of the hydrogel. The gel fraction (%) of SSH-*co*-MAA depended upon concentration of SSH, MAA, and MBA. The porosity (%) was increased with the increase in the concentration of SSH and decreased with the decrease in the concentration of MAA and MBA. The swelling indices, venlafaxine HCl loading, and release (24 h at the pH of the gastrointestinal tract) from VSSH-*co*-MAA were found to be dependent on the pH of the swelling media and the concentration of SSH, MAA, and MBA. The release of venlafaxine HCl followed non-Fickian diffusion mechanism. Conclusively, SSH-*co*-MAA is a novel material for potential application in targeted drug delivery applications.

Received 21st August 2022
Accepted 29th January 2023

DOI: 10.1039/d2ra05240g

rsc.li/rsc-advances

1. Introduction

Over the last two decades, the use of naturally occurring polysaccharides in various drug delivery systems (DDSs) has revolutionized the conventional dosage forms to novel and advanced DDSs. These polysaccharides are mostly plant-derived swellable biopolymers and are used as such in different DDSs or after chemical modifications to impart desired properties and increase the spectrum for biomedical applications.[1–3] Additionally, these swellable polysaccharides are biocompatible, biodegradable, non-immunogenic, non-toxic, cost-effective, and easily available.[4,5] Such attributes of the newly developed DDSs are very important to attain the sustainable development goals, *i.e.*, environmental, economic and social sustainability. Recently, these swellable and naturally occurring polysaccharide-based materials have shown stimuli-responsive swelling and de-swelling properties under various biological fluids as well as sustained and targeted drug delivery.[6,7] These polysaccharide-based materials are nowadays being converted into graft copolymeric hydrogels using various techniques for tissue engineering, wound healing, sustained drug release, and topical applications.[8–10]

Salvia spinosa is a plant in the Lamiaceae family and grows in the Mediterranean and phytogeographic regions of Saharo-Arabian.[11,12] The plant as a whole is enriched with different phytochemicals including flavonoids, terpenoids, fatty acids, coumarins, and phenolic acids.[13] The seed production capacity of each mature plant of *S. spinosa* is 1500 to 10 000.[12] The *S. spinosa* seeds have been utilized for the treatment of urinary tract infections, gonorrhea, and internal inflammation.[14] The mucilage, *i.e.*, *S. spinosa* hydrogel (SSH) released from its seeds is superporous, hemocompatible, non-toxic, thermally stable,

[a]*Institute of Chemistry, University of Sargodha, Sargodha 40100, Pakistan*
[b]*Faculty of Pharmacy, University of Sargodha, Sargodha 40100, Pakistan*
[c]*Centre for Organic Chemistry, School of Chemistry, University of the Punjab, Lahore 54590, Pakistan. E-mail: majaz172@yahoo.com*
[d]*Department of Chemistry, GC University, Lahore 54000, Pakistan*
[e]*Department of Chemistry, College of Science, Southern University of Science and Technology, Shenzhen, 518055, China*
[f]*Department of Chemistry, SBA School of Science & Engineering, Lahore University of Management Sciences, Lahore Cantt. 54792, Pakistan*
[g]*Department of Pharmaceutics, College of Pharmacy, Jouf University, Aljouf, Sakaka 72388, Saudi Arabia*

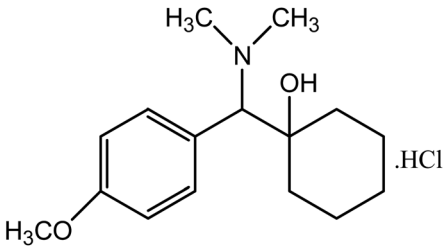

Fig. 1 Structure of venlafaxine HCl.

chemically modifiable, and has been utilized for the zero-order drug delivery application.[7,15,16]

Methacrylic acid (MAA) has been extensively used in the fabrication of pH-sensitive hydrogels. MAA is a pH-sensitive material and demonstrates extreme variations in swelling behavior when there is a change in pH and ionic strength. Its pH-sensitive behavior makes it a very significant material in temporal or spatial delivery, sustained release DDSs, and using diverse categories of drug moieties. By grafting the natural polysaccharides with synthetic monomers like MAA, properties of both entities (natural polysaccharides and MAA) could be achieved.[17] Venlafaxine HCl is an antidepressant drug of third generation. It is highly water-soluble with a short half-life of 4 h and more than 90% can absorb after oral administration. Venlafaxine HCl (Fig. 1) has been utilized for the treatment of depression, anxiety, and social phobia.

In the present research, we aimed to design a novel hydrogel network (SSH-*co*-MAA) comprises of a naturally occurring polysaccharide, *i.e.*, SSH with the help of MAA through free radical graft copolymerization. Aim is to characterize the SSH-*co*-MAA using Fourier transform infrared (FTIR) and solid-state NMR (CP/MAS ^{13}C-NMR) spectroscopy. Interest is to study the superporous nature of the SSH-*co*-MAA *via* SEM in order to access the potential of water uptake by the gel. We are also reporting on the evaluation of the effect of the concentration of polymer, *i.e.*, SSH; monomer, *i.e.*, MAA; and cross-linker, *i.e.*, MBA on the swelling properties of SSH-*co*-MAA, drug loading onto SSH-*co*-MAA, and venlafaxine HCl release behavior from venlafaxine HCl loaded SSH-*co*-MAA (VSSH-*co*-MAA) at different pH of the gastrointestinal tract (GIT), *i.e.*, pH 1.2, 4.5, 6.8 and 7.4.

2. Experimental

2.1. Materials

Seeds of *S. spinosa* were brought from the local market of Sargodha, Pakistan (in May–June) and their taxonomy was verified by a botanist, Dr Hassan Sher from the Department of Botany, University of Swat, Mingora, Pakistan. The methacrylic acid (MAA, monomer; 99.0%), potassium persulfate (KPS, initiator; 99.0%), and *N*,*N*-methylenebisacrylamide (MBA, cross-linker; 99.5%) were purchased from Sigma-Aldrich, Germany. Potassium dihydrogen phosphate (KH_2PO_4; 99.0%), NaOH (98.0%), KCl (99.0%), ethanol (95.0%), and *n*-hexane (95.0%) were acquired from Riedel-de Haen, Germany. Venlafaxine HCl (United States Pharmacopeia (USP) standard) was used as a model drug for *in vitro* drug release studies from the synthesized hydrogel carrier. For swelling and drug release studies, the buffers of pH 7.4, 6.8, 4.5, and 1.2 were prepared according to the procedure given in USP. All other reagents and chemical ingredients were of lab-grade. Deionized water (DW) was used during the whole research work.

2.2. Extraction of mucilage

To isolate the mucilage from the seeds of *S. spinosa*, the seeds (1 : 25 w/v, seed-water ratio) were soaked in DW for 2.5 h at 50 °C. Mucilage released from swollen seeds of *S. spinosa* was isolated by placing them between two layers of muslin cloth and rubbing with a spatula. The isolated mucilage was washed with DW and *n*-hexane in replicates to remove the impurities. The obtained mucilage was centrifuged to get the sediment paste and then dried in a vacuum oven at 50 °C. Dried hydrogel-able material was milled to get a powder, passed through a sieve no. 60, and stored in a desiccator after labeling as *S. spinosa* seeds mucilage (SSH) for further use in the experimental work. The images of the seeds, swollen seed in DW and dried milled SSH are shown in Fig. 2.

2.3. Synthesis of SSH-*co*-MAA

The free radical copolymerization reaction was used to synthesize novel composite hydrogel based on SSH and MAA. KPS was used as an initiator to generate free radicals on SSH and MAA. MBA was used to cross-link both precursors. An already

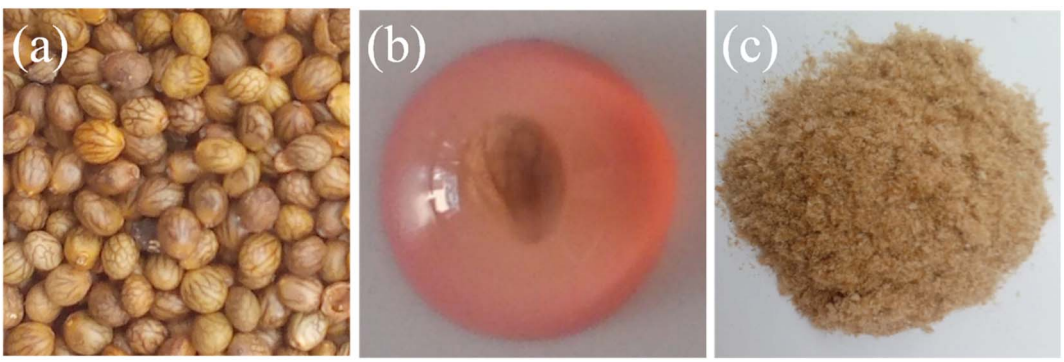

Fig. 2 Images of the seeds of *S. spinosa* (a), water swollen *S. spinosa* seed (red color is due to staining with permitted red food color) (b), and dried SSH isolated from the seeds of *S. spinosa* (c).

Table 1 Composition detail for the synthesis of SSH-*co*-MAA formulations

Formulation code	SSH (%, w/w)	MAA (%, w/w)	MBA (% mole ratio of monomer)	KPS (% mole ratio of monomer)
M1	1.5	35.0	0.4	0.4
M2	2.0	35.0	0.4	0.4
M3	2.5	35.0	0.4	0.4
M4	2.5	30.0	0.4	0.4
M5	2.5	32.5	0.4	0.4
M6	2.5	37.5	0.4	0.4
M7	2.5	35.0	0.6	0.4
M8	2.5	35.0	0.8	0.4
M9	1.5	35.0	1.0	0.4

reported method with slight modification was followed to synthesize SSH-*co*-MAA.[18] Briefly, after a number of trials (not reported here), 1.5% (w/w) of SSH, 35.0% (w/w) of MAA, 0.4% (w/w) of MBA, and 0.4% (w/w) of KPS was found preliminarily ideal concentrations for the synthesis of SSH-*co*-MAA. Based on these concentrations, nine different formulations of SSH-*co*-MAA were synthesized by changing the concentrations of SSH, MAA, and MBA. The composition of all formulations of SSH-*co*-MAA is incorporated in Table 1.

As a typical example, the procedure to synthesize the formulation M4 is reported. SSH (2.5%, w/w) was added in DW and vigorously stirred for 30 min at 70 °C. To the obtained mixture, KPS was added and the reaction was further continued for 15 min to generate free radicals on SSH. Later, the mixture was sonicated before cooling at room temperature and labeled as mixture "A". The solution "B" was prepared by dissolving MBA (0.4%, w/w) in MAA (30.0%, w/w) at room temperature. The mixture A and solution B were mixed and stirred for 30 min at room temperature. The final mixture was shifted to a test tube and heated at different temperatures for a specific time period, *i.e.*, for 1 h at 40 °C, 50 °C, 60 °C, and 70 °C, and then for 4 h at 80 °C in an electrical water bath to carry out copolymerization of SSH and MAA. Hydrogel (SSH-*co*-MAA) formed inside the test tube after 8 h was separated by cooling it at room temperature and then cut into discs of 4–6 mm size using a sharp blade. The discs of SSH-*co*-MAA were initially washed with DW and then with the mixture of DW and ethanol (70/30%, v/v) to eliminate the unreactive MAA. Finally, the SSH-*co*-MAA discs were dried in an oven at 60 °C and stored in an airtight vessel under a vacuum for further experimentations. The formulation M4 was used further for structural characterization.

2.4. Characterization

2.4.1. Spectroscopic characterization. SSH and SSH-*co*-MAA were characterized by recording their Fourier-transform infrared (FTIR) spectra on IR Prestige-21 spectrometer (Shimadzu, Japan) in the range of 4000–400 cm^{-1} using KBr pellet method. After loading the venlafaxine HCl onto SSH-*co*-MAA, the FTIR spectra of venlafaxine HCl and VSSH-*co*-MAA were also recorded to check the compatibility between them. Moreover, the solid-state CP/MAS ^{13}C-NMR spectrum of SSH-*co*-MAA was recorded on a Bruker DRX-400 machine at the ambient temperature for the confirmation of grafting of MAA onto SSH.

2.4.2. PXRD analysis. The PXRD pattern of SSH-*co*-MAA, venlafaxine HCl, and VSSH-*co*-MAA were recorded at the angle ranged from 0–50° on Xpert pro-analytical instrument. The scanning rate was maintained as 1° min^{-1} at 2θ. From the PXRD pattern, the physical changes corresponding to the fluctuation in the crystallinity pattern of the venlafaxine HCl were studied.

2.4.3. Thermal analysis. The thermogravimetric analysis of SSH-*co*-MAA and VSSH-*co*-MAA (after venlafaxine HCl loading) was conducted. The thermograms (TG curves) were recorded from ambient temperature to 800 °C under nitrogen flow (100 cm^3 min^{-1}) by maintaining the heating rate at 10 °C min^{-1} on SDT Q600 thermal analyzer (TA Instruments, USA).

2.4.4. SEM analysis. SEM images of the SSH and SSH-*co*-MAA were captured along transverse and longitudinal cross-sections to study the changes in the surface morphology of SSH after copolymerization with MAA. The dried discs of SSH-*co*-MAA were soaked in DW and allowed to swell. The swollen discs of SSH-*co*-MAA were freeze-dried and cut to transverse and longitudinal cross-sections with the help of a sharp blade. A sputter coater (Denton, Desk V HP) was used to coat gold on the cross-sections. The SEM images of the SSH and SSH-*co*-MAA were then captured on Scanning Electron Microscope (SEM; Nova, NanoSEM 450) at different magnifications.

2.5. Swelling studies of the SSH-*co*-MAA

2.5.1. pH-responsive dynamic and equilibrium swelling. At four different physiological pH of the GIT, *i.e.*, pH 1.2, 4.5, 6.8, and 7.4, the dynamic and equilibrium swelling responses of all formulations of the SSH-*co*-MAA were studied using the gravimetric method.[19] The pre-weighed discs of SSH-*co*-MAA were immersed in separate beakers having buffers (100 mL) of different pH at room temperature. The beakers were kept in a shaking incubator (JSSI-100C, JS Research Inc. Republic of Korea) and SSH-*co*-MAA discs were allowed to swell. After predefined time intervals, the swollen SSH-*co*-MAA discs were taken out from buffers, blotted with filter paper, accurately weighed, and swelling indices in terms of *Q* were calculated using eqn (1). For the determination of ES (eqn (2)), the SSH-*co*-MAA were swelled completely (for 7 days) in the corresponding buffers. The fully swollen SSH-*co*-MAA discs were then removed from the swollen media and weighed. Experiments regarding *Q* and ES were conducted in triplicate and the average of the values are reported here.

$$Q = \frac{W_s}{W_d} \quad (1)$$

$$ES = \frac{(M_{eq} - M_o)}{M_{eq}} \quad (2)$$

where, W_s shows the mass (g) of swollen SSH-*co*-MAA at time t, W_d is the mass (g) of dry SSH-*co*-MAA at $t = 0$, M_{eq} represents the mass (g) of swollen SSH-*co*-MAA at equilibrium and M_o is the initial mass (g) of SSH-*co*-MAA in dry form.

2.5.2. Swelling kinetics. The swelling data calculated according to eqn (1) was put into eqn (3) and (4) to measure the values of normalized degree of swelling (Q_t) and normalized equilibrium degree of swelling (Q_e), respectively. Later, the values of Q_t and Q_e were fed into a second-order kinetic equation (eqn (5)) and the rate at which SSH-*co*-MAA swelled was determined.

$$Q_t = \frac{W_s - W_d}{W_d} = \frac{W_t}{W_d} \quad (3)$$

$$Q_e = \frac{W_\infty - W_d}{W_d} = \frac{W_e}{W_d} \quad (4)$$

$$\frac{t}{Q_t} = \frac{t}{Q_e} + \frac{1}{kQ_e^2} \quad (5)$$

where, W_s is the mass (g) of the SSH-*co*-MAA in the swollen form at time t, W_d is the mass (g) of the SSH-*co*-MAA in dry form at time $t = 0$, and W_t indicates the mass (g) of buffer retained into the SSH-*co*-MAA at time t, W_∞ represents the mass (g) of the swollen SSH-*co*-MAA at time t_∞, and W_e is the mass (g) of buffer retained in the SSH-*co*-MAA at time $t = \infty$.

Graphs between the values of t/Q_t *vs.* t were plotted for swelling kinetic studies. From the obtained straight lines, the values of slope ($1/Q_e$), intercept ($1/kQ_e^2$), and regression coefficient (R^2) were calculated.

2.5.3. Swelling and de-swelling (on-off switching) studies. To determine the swelling and de-swelling properties of SSH-*co*-MAA in basic (pH 7.4; swelling media) and acidic (pH 1.2; de-swelling media) environments, three formulations, *i.e.*, M3, M4, and M7 were selected because of having maximum swelling. The pre-weighed SSH-*co*-MAA discs of these three formulations were first swelled in the buffer of pH 7.4 for 72 h and then transferred to a buffer of pH 1.2 for de-swelling study, *i.e.*, for 80 min. The weight of SSH-*co*-MAA (swelled and de-swelled form) was determined accurately using eqn (1) during the swelling and de-swelling phases. The results were graphically represented after recording the four consecutive cycles of swelling and de-swelling.

2.6. Determination of sol–gel fraction

The determination of the sol–gel fraction will provide information about the extent of the degree of cross-linking between the SSH and MAA. To determine sol–gel fraction the procedure described in the literature was adopted with necessary modification.[20] Briefly, after the synthesis of SSH-*co*-MAA, the dry and un-washed SSH-*co*-MAA discs of every formulation were soaked in a mixture of DW and ethanol (70/30%, v/v) and placed on a shaking incubator for 48 h at ambient temperature. Later, the SSH-*co*-MAA discs were taken out from the soaking media, cleaned with filter paper, dried in an oven at 50 °C, and weighed to determine sol and gel fractions using eqn (6) and (7), respectively.

$$\%\ \text{sol fraction} = \frac{W_i - W_s}{W_i} \times 100 \quad (6)$$

$$\%\ \text{gel fraction} = 100 - \text{sol fraction} \quad (7)$$

where, W_i is the initial weight of SSH-*co*-MAA and W_s is the dried weight (g) of SSH-*co*-MAA after soaking in a mixture of DW and ethanol.

2.7. Porosity measurement

The solvent displacement method was used to determine the porosity of SSH-*co*-MAA in percentage.[21] Briefly, the pre-washed SSH-*co*-MAA discs were weighed, dipped in ethanol (100 mL) for 24 h, and then weighed again after blotting surface ethanol with filter paper. The porosity was measured using eqn (8).

$$\%\ \text{porosity} = \frac{M_2 - M_1}{\rho V} \times 100 \quad (8)$$

where, M_2 is the mass (g) of SSH-*co*-MAA after soaking in ethanol, M_1 is the initial mass (g) of SSH-*co*-MAA in dry form, ρ is the density (g cm^{-3}) of absolute ethanol, and V is the volume (cm^3) of SSH-*co*-MAA after soaking in the ethanol for 24 h.

2.8. Drug release studies from VSSH-*co*-MAA

2.8.1. Drug loading onto SSH-*co*-MAA. For drug loading, fresh venlafaxine HCl solution (1%, w/v) was prepared in the buffer of pH 7.4 and the weighed SSH-*co*-MAA discs were soaked in this solution for 24 h. After that, venlafaxine HCl loaded SSH-*co*-MAA, *i.e.*, VSSH-*co*-MAA was blotted with filter paper to clean its surface from surplus solution, put in an oven at 50 °C to dry till constant weight, and weighed again.

The drug loading capacity of SSH-*co*-MAA was determined using gravimetric and extraction methods.[22] For the gravimetric method, the amount of drug loading was determined using eqn (9).

$$\text{Amount of drug loaded} = W_D - W_d \quad (9)$$

where, W_D is the weight (mg) of dried VSSH-*co*-MAA and W_d is the weight of dried SSH-*co*-MAA.

Secondly, a repeated extraction method was employed to determine the amount of venlafaxine HCl loaded onto the SSH-*co*-MAA. The dried discs of VSSH-*co*-MAA were immersed in a freshly prepared buffer of pH 7.4 (100 mL) for 24 h at room temperature. Then VSSH-*co*-MAA was removed from the buffer and the remaining buffer was first filtered to remove undesired particles, sonicated for 30 min and the venlafaxine HCl concentration was determined through UV-vis spectrophotometer (UV-1600 Shimadzu Germany) at 274 nm. The VSSH-*co*-MAA was re-immersed in the same freshly prepared buffer and the

whole process was continued until all the contents of entrapped venlafaxine HCl were removed from the VSSH-*co*-MAA discs. The venlafaxine HCl loading was calculated using the calibration curve method.

2.8.2. *In vitro* drug release studies. A dissolution study was conducted on USP Dissolution Apparatus II (Pharma Test, Germany) at 37 ± 0.5 °C and 50 rpm to evaluate the *in vitro* release of drug from VSSH-*co*-MAA. The drug release from VSSH-*co*-MAA was observed in conditions that mimic the transit time and pH of GIT using the pH-change method. Therefore, the VSSH-*co*-MAA was placed at pH 1.2 for 2 h, at pH 4.5 for 3 h, at pH 6.8 for 7 h, and at pH 7.4 for the next 12 h. Although, this method is very useful to know the effect of pH on drug release, however, the drug release kinetics and mechanism involved in the release could not be determined by the pH change method. Therefore, the drug release behavior from VSSH-*co*-MAA was also studied in the buffers of pH 1.2, 4.5, 6.8, and 7.4 for 24 h. For the dissolution study, the VSSH-*co*-MAA was dipped in the vessel having respective dissolution media (900 mL). An aliquot of the sample (10 mL) was pipetted out after pre-defined time intervals and the dissolution media was restored by adding the same amount of freshly prepared buffers. The withdrawn sample was filtered, sonicated, and necessary diluted before analyzing through UV-vis spectrophotometer at 274 nm. The cumulative venlafaxine HCl release was determined in percentage using eqn (10).

$$\%\ \text{drug release} = \frac{F_t}{F_{\text{loaded}}} \times 100 \tag{10}$$

where, F_t is the amount of venlafaxine HCl released from VSSH-*co*-MAA after time t and F_{loaded} is the net amount of venlafaxine HCl loaded onto SSH-*co*-MAA.

2.8.3. Drug release kinetics and mechanism. The venlafaxine HCl release data was put into the zero-order (eqn (11)), first-order (eqn (12)), Hixson-Crowell (eqn (13)), Higuchi (eqn (14)), and Korsmeyer–Peppas (eqn (15)) kinetic models to determine the kinetics and mechanism of venlafaxine HCl release from VSSH-*co*-MAA.

$$Q_t = K_0 t \tag{11}$$

where, Q_t shows the amount of venlafaxine HCl release after any time t and K_0 is the zero-order rate constant.

$$\log Q = \log Q_0 - \left(\frac{K_1 t}{2.303}\right) \tag{12}$$

where, Q_0 is the amount of venlafaxine HCl loaded onto the SSH-*co*-MAA, Q is the amount of venlafaxine HCl that have to be released, K_1 is the first-order rate constant, and t is the time at which aliquot is given out from dissolution media.[23]

$$Q_0^{1/3} - Q_t^{1/3} = -K_{\text{HC}} t \tag{13}$$

where, Q_0 represents the amount of venlafaxine HCl to be released from VSSH-*co*-MAA, Q_t is the net amount of venlafaxine HCl released after time t, and K_{HC} is the Hixson–Crowell rate constant.[24]

$$Q_t = K_{\text{H}}(t^{1/2}) \tag{14}$$

where, Q_t is the amount of venlafaxine HCl released from VSSH-*co*-MAA after time t and K_{H} is the Higuchi model rate constant.[25]

$$\frac{M_t}{M_\infty} = k_{\text{p}} t^n \tag{15}$$

where, M_t/M_∞ represents the amount of venlafaxine HCl that is released after time t, k_{p} is the Korsmeyer–Peppas model rate constant, and n indicates the diffusion exponent. The value of n helps in determining the venlafaxine HCl release mechanism. Its value may be less than 0.45, between 0.45–0.89, or greater than 0.89 for Fickian diffusion, non-Fickian diffusion, and super case-II transport, respectively.[26,27]

The Model Selection Criterion (MSC), *i.e.*, a modified Akaike information criterion was also applied to the venlafaxine HCl release data and the information regarding appropriate release kinetics models was acquired using eqn (16).[28] MSC is considered independent of the scaling of data points. Moreover, the kinetics model having the highest value of MSC is recognized as the best fit model.

$$\text{MSC} = \ln\left(\frac{\sum_{i=1}^{n} w_i\left(Y_{\text{obs}_i} - \overline{Y}_{\text{obs}}\right)^2}{\sum_{i=1}^{n} w_i\left(Y_{\text{obs}_i} - Y_{\text{cal}_i}\right)^2}\right) - \frac{2p}{n} \tag{16}$$

where, Y_{obsi} represents the observed value of i^{th} data point, Y_{cali} is the calculated value of i^{th} data point, $\bar{Y}_{\text{obs}}$ is the mean of observed data points, w_i is the optional weight factor, p is the number of parameters and n is the number of data points.

3. Results and discussion

3.1. Synthesis of SSH-*co*-MAA and reaction mechanism

Using the free radical copolymerization method, SSH and MAA-based novel composite hydrogel, *i.e.*, SSH-*co*-MAA (nine different formulations) was synthesized. Fig. 3 is showing the involvement of a three-step mechanism, such as initiation, propagation, and termination in the synthesis of SSH-*co*-MAA. In the first step, the peroxide bond (–O–O–) in the initiator (KPS) was homolytically decomposed to sulfate anion free radicals ($SO_4^{\bullet -}$) upon heating at 70 °C. These $SO_4^{\bullet -}$ reacted with DW and produce hydroxyl radicals ($-OH^{\bullet -}$) which intern generated free radicals on SSH by removing protons of its hydroxyls and designated as SSH–$O^{\bullet -}$. Moreover, the $SO_4^{\bullet -}$ homolytically cleaved the pi-bond of vinyl linkage of MAA and converted it to the free radicals, *i.e.*, OH–$CH_2C^{\bullet -}(CH_3)$–COOH. In the propagation step, the OH–$CH_2C^{\bullet -}(CH_3)$–COOH is self-polymerized to produce poly(MAA) which is further grafted onto SSH and developed persulphate-saccharide redox system (macro-biradical I). As the cross-linker (MBA) has two unsaturated double bonds, therefore, it provided four reactive sites. Therefore, MBA linked with macro-biradical I and converted it to macro-biradical II. Lastly, in the termination step, macro-biradical II coupled and produced SSH-*co*-MAA as illustrated in Fig. 3.[29]

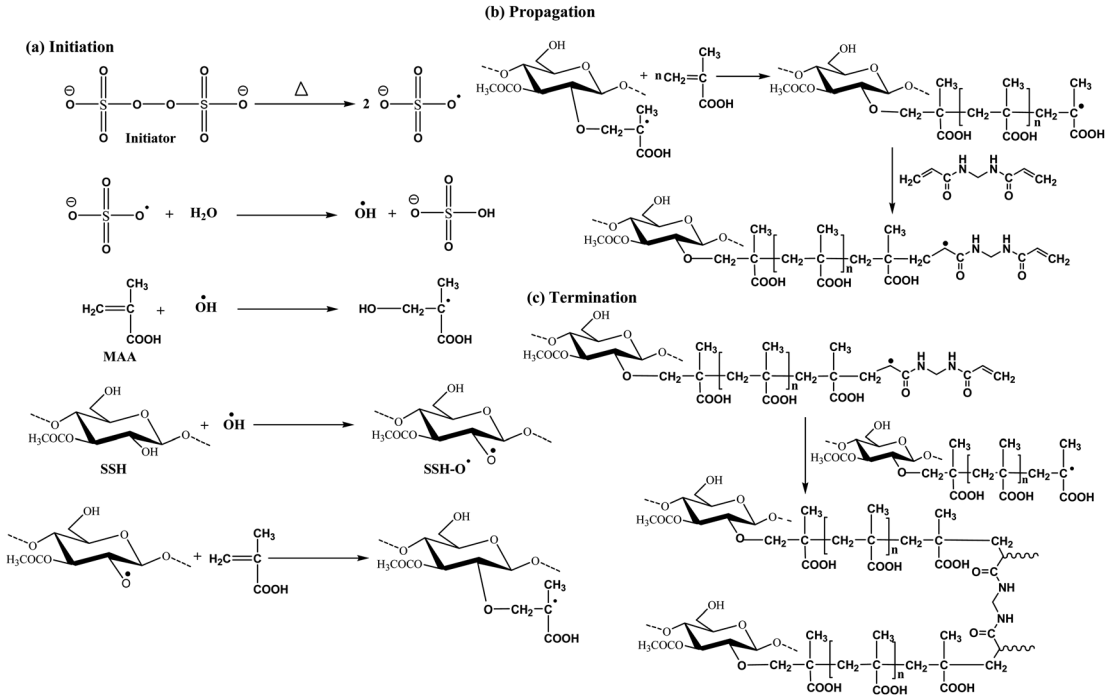

Fig. 3 Illustrated free radical reaction scheme for the synthesis of SSH-*co*-MAA.

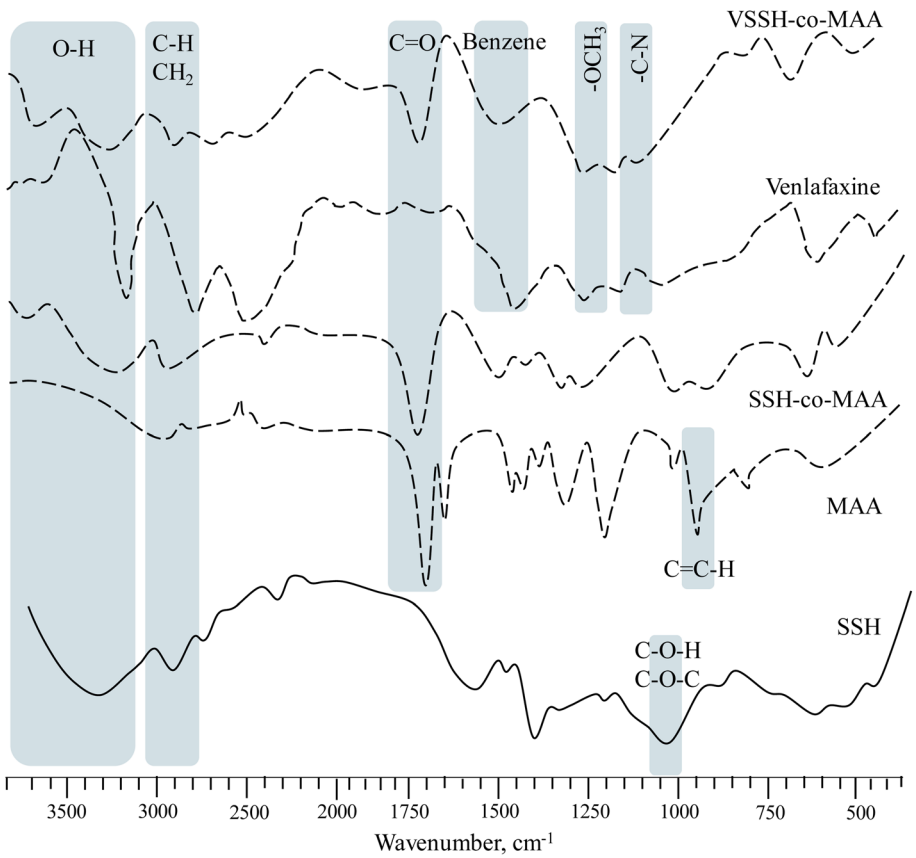

Fig. 4 Overlay FTIR spectra of SSH, MAA, SSH-*co*-MAA, venlafaxine HCl, and VSSH-*co*-MAA. FTIR spectrum of venlafaxine HCl is reprinted from (ref. 33) with permission from Elsevier.

3.2. Characterization

3.2.1. FTIR analysis. Fig. 4 is showing the overlay FTIR spectra of SSH, MAA, SSH-*co*-MAA, venlafaxine HCl, and VSSH-*co*-MAA. A peak at 2987 cm^{-1} due to the vibration of H in CH_2=C(CH_3)–COOH, and a strong and sharp peak corresponding to C=O stretching at 1692 cm^{-1} appeared in the FTIR spectrum of MAA. A signal at 944 cm^{-1} due to vinyl linkage (C=C–H) can also be seen in its spectrum.[30] After conversion, a broadband at 2987 cm^{-1} in the spectrum of MAA is not present in the spectrum of SSH-*co*-MAA, it is because of conversion of unsaturated pi-bond of MAA to saturated sigma-bond after the copolymerization. Likewise, the spectrum of MAA contains a peak at 944 cm^{-1} while the same peak in the spectrum of MAA became weaker and slightly shifted to a lower wavenumber, *i.e.*, 937 cm^{-1}. A peak at 1722 cm^{-1} (CO) in the spectrum of SSH-*co*-MAA also appeared. Besides, the peaks for glycosidic linkages (COC) at 1188 cm^{-1} and CH in the methylene group at 1469 cm^{-1} were also observed in the spectrum of SSH-*co*-MAA.[31] Therefore, all of this evidence supported the successful grafting of MAA onto the SSH backbone.

A peak at 1269 cm^{-1} in the spectrum of venlafaxine HCl corresponds to the stretching vibrations of the methoxy group (OCH_3). The peak for CN can also be seen in the spectrum at wavenumber ranging from 1197–1147 cm^{-1}. Also, the peaks at 1469 and 3323 cm^{-1} indicate the presence of benzene ring and OH, respectively in the venlafaxine HCl.[32] The spectrum of VSSH-*co*-MAA has all the vital bands of venlafaxine HCl and SSH-*co*-MAA as described earlier without any significant alteration in their band shifting or the appearance of new bands. Hence, indicated that the venlafaxine HCl was successfully loaded onto SSH-*co*-MAA without producing any chemical change between them.

3.2.2. Solid-state CP/MAS ^{13}C-NMR analysis. The solid-state CP/MAS ^{13}C-NMR spectrum of SSH-*co*-MAA is presented in Fig. 5a. After copolymerization of SSH with MAA, the signals of C=O appeared at 182.50 ppm whereas the signals due to CH_2 and CH of MAA was observed at 45.28 ppm. The distinct signal of CH_3 of MAA in SSH-*co*-MAA appeared at 17.69 ppm. After copolymerization, the major portion in SSH-*co*-MAA is MAA, therefore all signals of the sugar region of SSH are generally difficult to observe in the NMR spectrum of SSH-*co*-MAA. However, the long signals of C2-6 are yet therein the spectrum of SSH-*co*-MAA and are detectable. For reference, the spectrum of SSH is given elsewhere.[15]

3.2.3. PXRD analysis. Powder X-ray diffraction analysis is used to determine the crystallinity/amorphous nature of the polymers. The PXRD diffractograms of SSH-*co*-MAA, venlafaxine HCl, and VSSH-*co*-MAA are shown in Fig. 5b. The PXRD graph of venlafaxine HCl showed sharp peaks at 20.5°, 21.3°, 21.9° and 25.2° due to its crystalline nature.[33] Though, the diffractogram of VSSH-*co*-MAA displayed subtle peaks instead of sharp peaks indicating that the venlafaxine HCl was present in an amorphous form in the formulated VSSH-*co*-MAA.[37] Moreover, the diffused nature of the peaks of VSSH-*co*-MAA confirmed the entrapment of the venlafaxine HCl in the chemically cross-

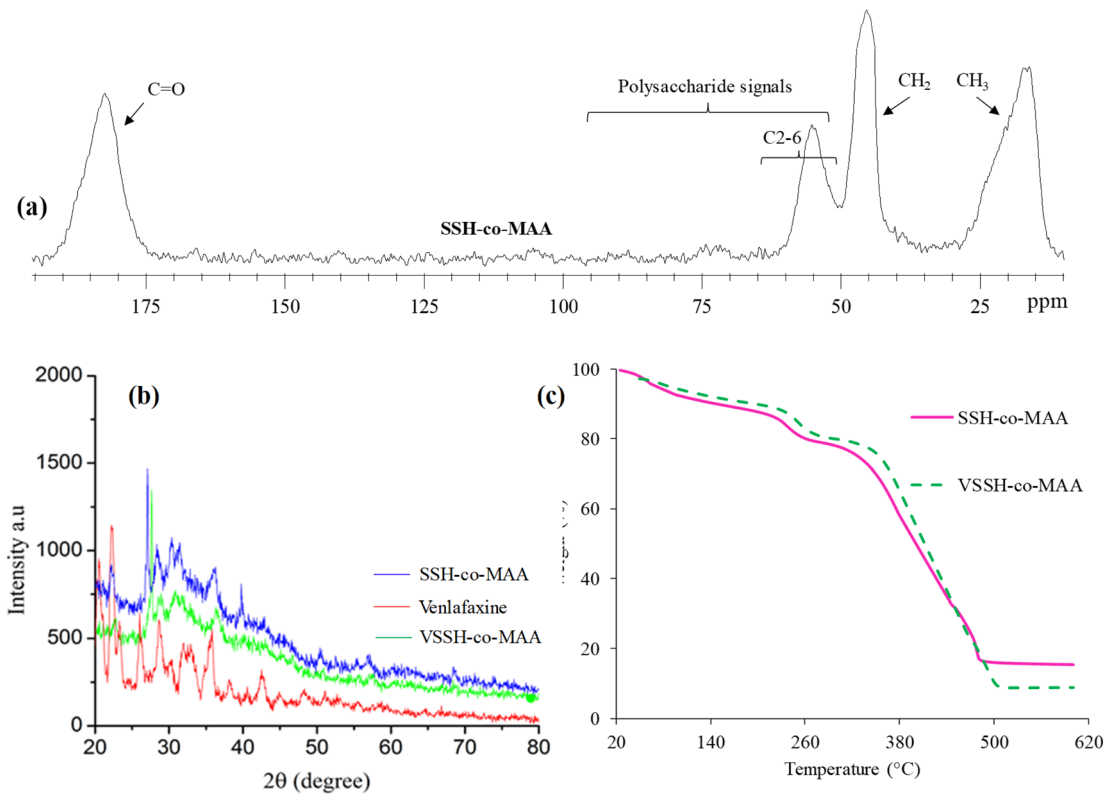

Fig. 5 Solid-state CP/MAS ^{13}C-NMR of SSH-*co*-MAA (a), overlay PXRD spectra of SSH-*co*-MAA, venlafaxine HCl, and VSSH-*co*-MAA (b), overlay TG curves of SSH-*co*-MAA, and VSSH-*co*-MAA (c). A figure portion ((b), PXRD spectrum of venlafaxine HCl) is reprinted from (ref. 33) with permission from Elsevier.

linked hydrogel network and the masking of the crystalline form of venlafaxine HCl. Furthermore, the crystallinity of venlafaxine HCl reduced subsequent its loading which is signal of efficacious encapsulation and diffusion at molecular level in hydrogel structure. As the amorphous form is more soluble than the crystalline form, the solubility of the drug was improved in synthesized hydrogel.

3.2.4. Thermal analysis. The overlay TG curves of SSH-*co*-MAA before and after drug (venlafaxine HCl) loading (VSSH-*co*-MAA) are presented in Fig. 5c and the corresponding thermal data calculated from the TG curve is presented in Table 2. The values of thermal decomposition of SSH-*co*-MAA are high and it degraded majorly in 350–500 °C range which is higher band even than the precursor, SSH.[15] Therefore, these findings indicated that the grafting of MAA onto SSH yielded thermally stable copolymer which expected to have higher shelf life hence, such materials can be stored over a long period of time. Furthermore, the loading of venlafaxine HCl onto SSH-*co*-MAA did not alter the stability of copolymer and *vice versa*.

Table 2 Thermal decomposition data of SSH-*co*-MAA, and VSSH-*co*-MAA[a]

Sample	Step	Td_i (°C)	Td_m (°C)	Td_f (°C)	Char yield (wt%)
SSH-*co*-MAA	I	205	249	290	15.37 at 600 °C
	II	320	470	490	
VSSH-*co*-MAA	I	230	255	300	8.86 at 600 °C
	II	330	482	505	

[a] SSH-*co*-MAA: *S. spinosa* mucilage and methacrylic acid copolymer hydrogel; VSSH-*co*-MAA: venlafaxine HCl loaded SSH-*co*-MAA.

3.2.5. SEM analysis. SEM images of the SSH (Fig. 6a and d) and SSH-*co*-MAA (Fig. 6b, c, e and f) indicated the porous surface and presence of interconnected channels in both the materials. The appearance of these pore and interconnected channels in SSH-*co*-MAA are might be due to the presence of the ionic and hydrophilic nature of the fundamental constituents including SSH and MAA. These constituents are responsible for the penetration of the solvent into SSH-*co*-MAA and lead to an increase in its hydrophilicity, swelling, and porosity. Hence, these channels are also further responsible for swelling and deswelling properties of SSH-*co*-MAA, loading of venlafaxine HCl onto SSH-*co*-MAA, and release of venlafaxine HCl from VSSH-*co*-MAA. On comparing, it was observed that the pore size of the SSH was greater than SSH-*co*-MAA which is evidenced by the histograms (Fig. 6g for SSH and Fig. 6h for SSH-*co*-MAA) but even the copolymer contains still a superporous nature.

3.3. Swelling studies of SSH-*co*-MAA

As the swelling properties of the hydrogel systems play a key role in the development of immediate as well as sustained release DDSs, therefore, it is important to evaluate the various factors that affect the swelling properties of the SSH-*co*-MAA.

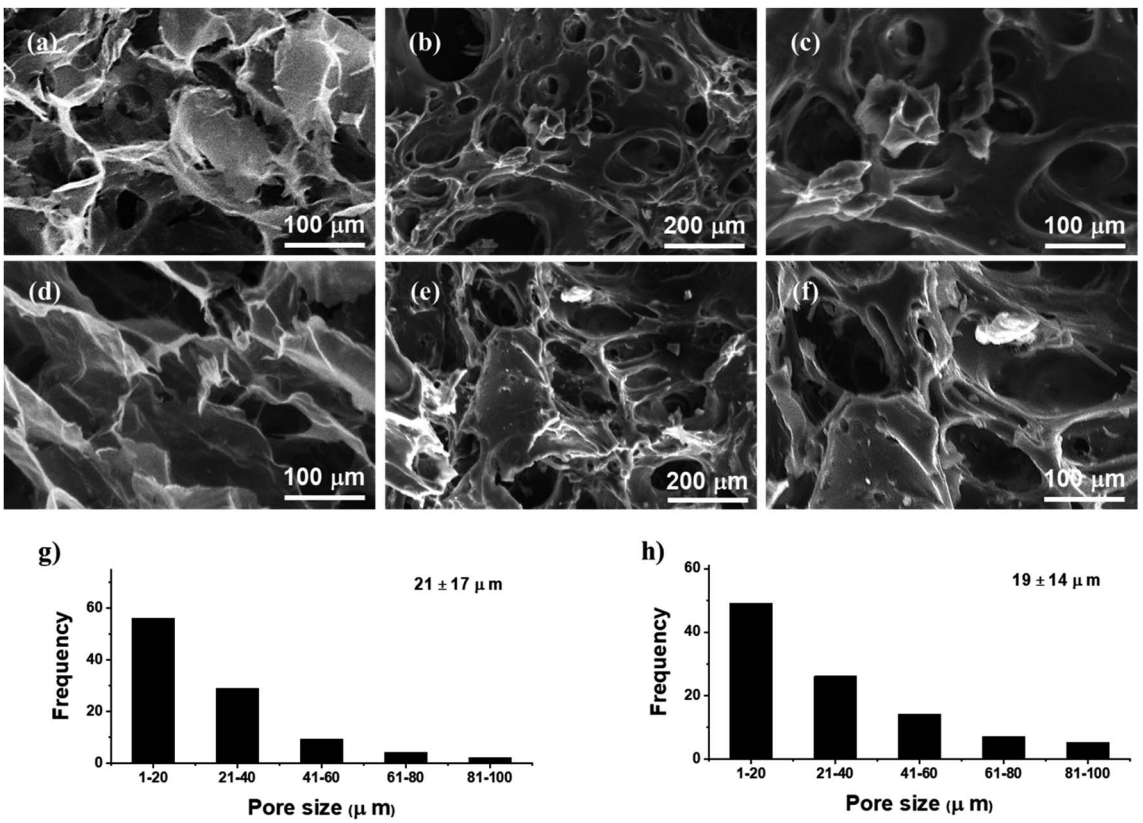

Fig. 6 Scanning electron micrographs of SSH transverse (a) and longitudinal (d), and SSH-*co*-MAA transverse (b and c) and longitudinal (e and f) cross-sections in swollen then freeze-dried form. Size distribution of macropores of SSH transverse (g) and SSH-*co*-MAA transverse (h) cross-sections.

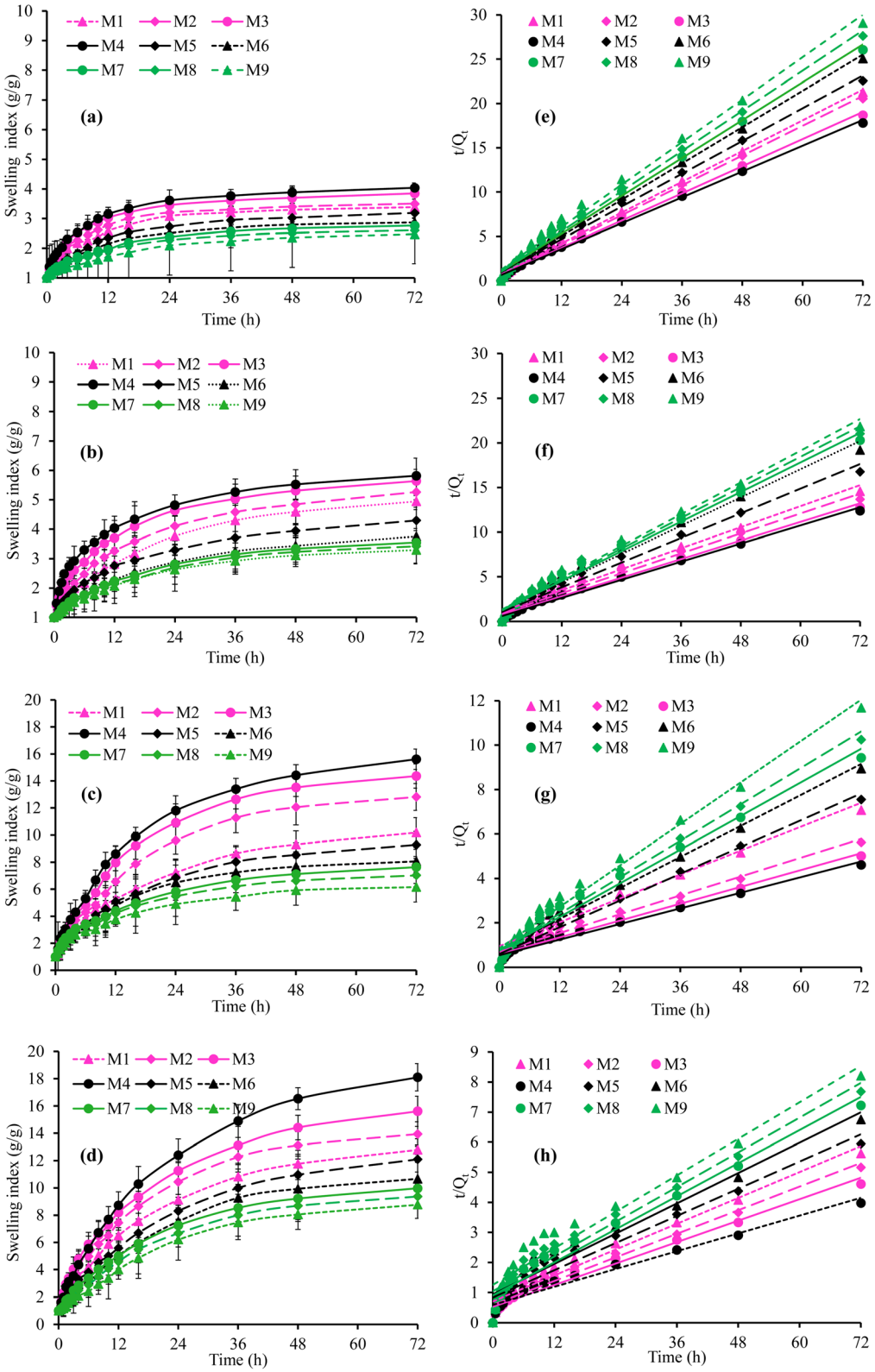

Fig. 7 Swelling index (g g^{-1}) and second-order swelling kinetics of SSH-*co*-MAA at pH 1.2 (a and e), pH 4.5 (b and f), pH 6.8 (c and g), and pH 7.4 (d and h).

3.3.1. Effect of pH. The graphical representation of the effect of different pH of GIT, such as pH 1.2, 4.5, 6.8, and 7.4 on the dynamic swelling indices and equilibrium swelling of the SSH-*co*-MAA is depicted in Fig. 7 and 8, respectively. The SSH-*co*-MAA showed maximum swelling at pH 7.4 (Fig. 7d) and least swelling at pH 1.2 (Fig. 7a). The overall swelling order of all the

formulations of SSH-*co*-MAA was found in the sequence of pH 7.4 > 6.8 > 4.5 > 1.2. The nearly off swelling of SSH-*co*-MAA at pH 1.2 is due to the protonation and association of the carboxylic acid (COOH) group of SSH. In response to protonation, the possible anion–anion (carboxylate–carboxylate) interactions are eliminated, and hydrogen bonding becomes strengthened due to which physical cross-linking between polymer chains may develop. Therefore, a decrease in the swelling index was observed at pH 1.2 (Fig. 7a).[34] However, as the pH of the swelling media was increased from pH 1.2 to pH 4.5 (Fig. 7b), 6.8 (Fig. 7c), and 7.4 (Fig. 7d), the COOH groups of SSH-*co*-MAA ionized to carboxylate anion (COO^-) by giving protons in the basic environment (pH 7.4). Consequently, electrostatic (anion–anion) repulsions between the polymer chains may develop which leads to an increase in the swelling. At pH 4.5, less swelling as compared to a buffer of pH 6.8 and 7.4 and more swelling as compared to a buffer of pH 1.2 was observed. At pH 4.5, a fewer number of ionizable COOH groups are present as compared to a buffer of pH 6.8 and 7.4 and a greater number of ionizable COOH groups are present as compared to a buffer of pH 1.2. Due to less number of ionizable COOH, penetration of liquid may hinder at pH 4.5 and result in the decrease of swelling.

For a better understanding of the pH-responsive swelling behavior of SSH-*co*-MAA, the mean of the swelling of all the formulations and corresponding swelling kinetic data was plotted and presented in Fig. 8a and b, respectively. Such studies revealed that SSH-*co*-MAA is a pH-responsive material and could be a suitable candidate for the designing of sustained and targeted DDSs.

3.3.2. Effect of polymer concentration. The concentration of SSH was varied from 1.5 to 2.5% to evaluate the effect of polymer concentration on the *Q* and ES of SSH-*co*-MAA at a constant concentration of MAA (35.0%), MBA (0.4%), and KPS (0.4%). The swelling of SSH-*co*-MAA was found directly related to the concentration of SSH. The formulation (M3) of SSH-*co*-MAA prepared using 2.5% SSH showed maximum swelling. In comparison, the order of swelling was found as M1 < M2 < M3 in all the swelling media (Fig. 7a–d for *Q* and Fig. 8c–e for ES). This trend is attributed to the polyelectrolyte nature of SSH and due to the presence of polar functional groups, like OH in SSH as evident from the FTIR (Fig. 4) and solid-state CP/MAS ^{13}C-NMR spectrum (Fig. 5a). Such functionalities are responsible for the increase in translational entropy of the counter ions and hydrophilicity which in turn increases the swelling responses. However, using more than 2.5% of SSH the swelling indices tend to decrease which may be due to the increase in the viscosity of the reaction mixture. Consequently, the viscosity of the reaction mixture was increased followed by the increased steric hindrance of ionic groups of SSH which restricted the free rotation of water molecules. Hence, swelling of the SSH-*co*-MAA tends to decrease. Therefore, the best formulation of SSH-*co*-MAA can be prepared using 2.5% SSH.

3.3.3. Effect of monomer concentration. At an optimum concentration of SSH (2.5%), MBA (0.4%), and KPS (0.4%), the effect of monomer (MAA) concentration on the *Q* and ES of the SSH-*co*-MAA was studied using 30.0 to 37.5% of MAA. The obtained results are graphically presented in Fig. 7a–d for *Q* and Fig. 8d for ES. It was revealed that with the increase in the concentration of MAA, the swelling of SSH-*co*-MAA tends to decrease abruptly up to its optimum concentration, *i.e.*, 30.0%. The order of swelling in buffers of pH 1.2, 4.5, 6.8, and 7.4 was found to be M4 > M5 > M6. The MAA is a hydrophilic monomer having ionize-able COOH groups, hence, increasing concentration in the reaction mixture increases the number of COOH groups in the hydrogel systems to be developed. Therefore, due to the increase in the concentration of the MAA, the swelling of the SSH-*co*-MAA should be increased. However, the presence of electron donor acetyl group (CH_3) in this monomer resulted in steric hindrance which consequently retarded the SSH-*co*-MAA to swell more. Therefore, a decrease in *Q* and ES of SSH-*co*-MAA was noted with an increase in the concentration of MAA.[18] Moreover, due to the increase in the concentration of MAA, the reaction mixture may become viscous which resulted in a highly cross-linked and less porous SSH-*co*-MAA. Due to less porosity, the ability of swelling media to penetrate the SSH-*co*-MAA was reduced.[18] Consequently, the swelling of SSH-*co*-MAA was found to be decreased at a higher concentration of MAA, *i.e.*, greater than 30.0%.

3.3.4. Effect of cross-linker concentration. The effect of increasing the concentration of the MBA on the *Q* and ES of SSH-*co*-MAA was also evaluated at 2.5% SSH, 35.0% MAA, and 0.4% KPS. The obtained results have revealed that by increasing the concentration of MBA from 0.4 to 1.0%, the *Q* and ES of the SSH-*co*-MAA decreased (Fig. 7a–d for *Q* and Fig. 8e for ES). This trend is because, on increasing the concentration of the MBA, the cross-linking density of the SSH-*co*-MAA may be increased which imparted more compactness, rigidity, and stability to the SSH-*co*-MAA. Therefore, SSH-*co*-MAA absorbs a small quantity of the swelling media, *i.e.*, buffers of pH 1.2, 4.5, 6.8, and 7.4 and less swelling of SSH-*co*-MAA was observed.[35] Moreover, due to the presence of the high amount of the MBA, the physical entanglement between the polymeric chains of SSH-*co*-MAA may increase due to which the SSH-*co*-MAA become more and more cross-linked as well as least acidic. Hence, the COOH groups of SSH-*co*-MAA get covered which did not allow the polymeric chains of SSH-*co*-MAA to move freely by imparting hydrophobicity to SSH-*co*-MAA and by slowing down the ionization process.[35] Hence, 0.4% of MBA appeared ideal amount of MBA for the synthesis of SSH-*co*-MAA.

3.3.5. Swelling kinetics. The swelling data obtained after swelling of all formulations of SSH-*co*-MAA at pH 1.2, 4.5, 6.8, and 7.4 was put in a second-order swelling kinetics model and depicted in Fig. 7e–h. Second-order swelling kinetics explained the swelling capacity of the polymer in terms of the rate of swelling in un-hydrated and hydrated form. Moreover, second-order swelling kinetics also established that the rate of swelling of a polymer or rate of absorbency of swelling media by the polymer is directly proportional to the polymer's capacity to convert into a hydrated or swollen form at a specific time.[36] Therefore, by considering the value of regression coefficient, *i.e.*, (R^2) approaching "1" is considered the best fitted kinetic equation or followed the second-order swelling kinetics.

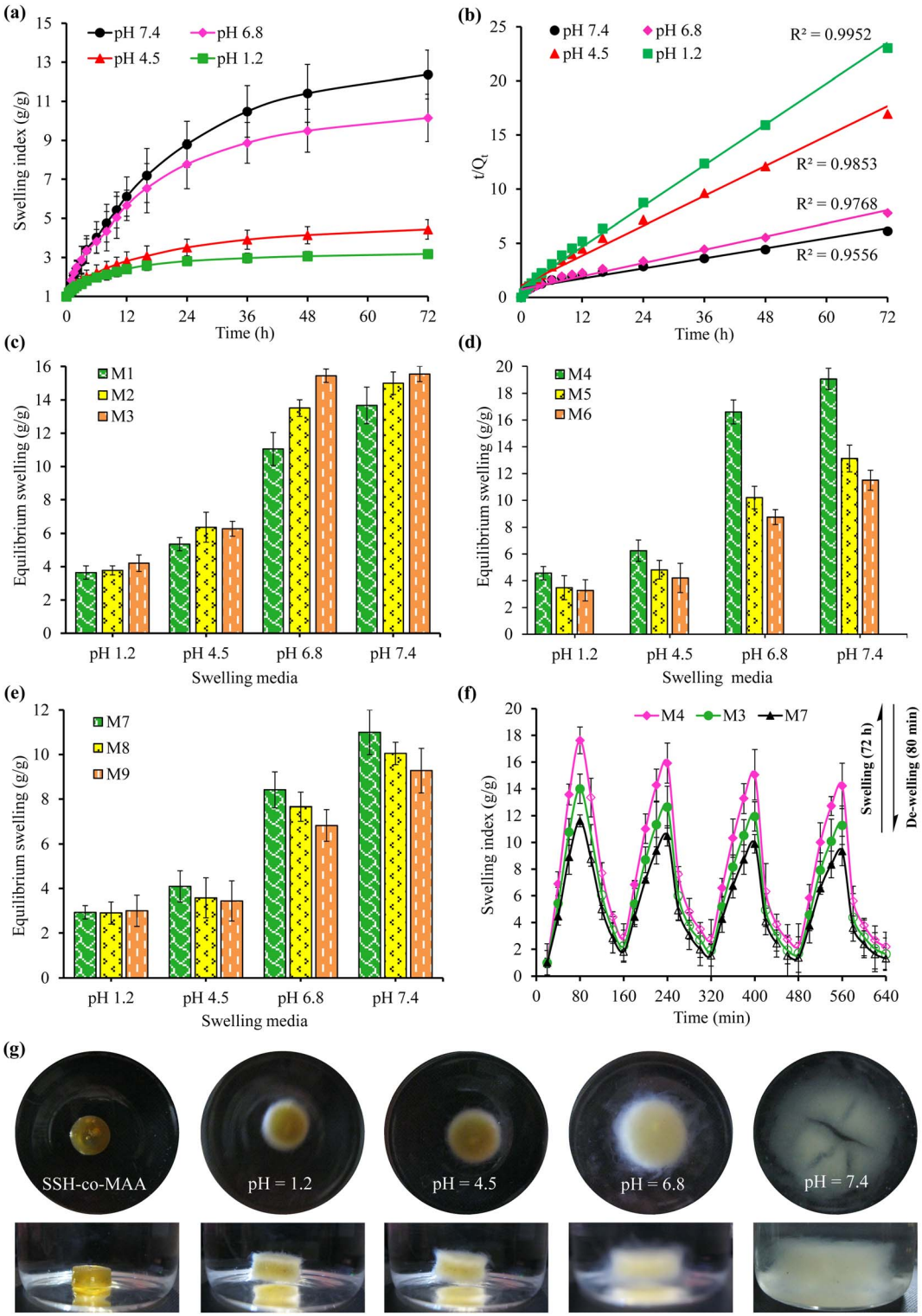

Fig. 8 Cumulative swelling index (g g^{-1}) (a) and swelling kinetics (b) of all formulations of SSH-*co*-MAA at pH 1.2, 4.5, 6.8, and 7.4, the effect of concentration of polymer (c), monomer (d), and cross-linker (e) on equilibrium swelling (g g^{-1}) of SSH-*co*-MAA at pH 1.2, 4.5, 6.8, and 7.4, swelling and de-swelling responses of formulations M3, M4, and M7 at pH 7.4 and 1.2 (f), and photographs of the swollen SSH-*co*-MAA at pH 1.2, 4.5, 6.8, and 7.4 captured after 72 h (g).

3.3.6. Swelling and de-swelling (on-off switching) studies of SSH-*co*-MAA. Three formulations, *i.e.*, M3, M4, and M7 were selected based on their high swelling indices to study the pH-responsive swelling and de-swelling properties of SSH-*co*-MAA in the buffer of basic pH (pH 7.4; swelling media) and acidic pH (pH 1.2; de-swelling media) at ambient temperature mimicking

the pH of the intestine and stomach, respectively. The rate of swelling of SSH-*co*-MAA discs was slow at pH 7.4, therefore, the SSH-*co*-MAA discs were kept in the swelling media for 72 h to swell completely. The fully swollen SSH-*co*-MAA discs were then transferred to the acidic buffer and rapid de-swelling was observed. This process of swelling and de-swelling of SSH-*co*-MAA was repeated four times and showed the pH-responsiveness of SSH-*co*-MAA as well as the reproducibility of the results (Fig. 8f). It was also observed that after each cycle of swelling and de-swelling, the swelling capacity of SSH-*co*-MAA decreased slightly. Before the start of the second swelling and de-swelling cycle, some portion of the de-swelling media (buffer of pH 1.2) remained in the swollen SSH-*co*-MAA which created a hindrance in the entrance of swelling media (buffer of pH 7.4) as well as the swelling of SSH-*co*-MAA up to the level of the first swelling cycle. Moreover, the swelling and de-swelling are due to the switching of the SSH-*co*-MAA between ionized (COO^-) and unionized (COOH) states of carboxylic groups.[37] Hence, the findings of pH-responsive swelling and de-swelling of SSH-*co*-MAA indicated that SSH-*co*-MAA could be an ideal material for developing a pH-responsive sustained release DDSs. The images of optimized formulation (M4) captured during swelling at pH 7.4 (Fig. 9c) and after complete swelling (after 72 h) at pH 1.2, 4.5, 6.8, and 7.4 (Fig. 8g) indicated the pH-dependent swelling of SSH-*co*-MAA.

3.4. Determination of sol–gel fraction

To determine the amount of uncross-linked soluble and cross-linked insoluble components in the gel structure of SSH-*co*-MAA, the fractions of sol and gel were determined. A direct relationship between gel-fraction and the concentration of SSH, MAA, and MBA in SSH-*co*-MAA was observed, *i.e.*, by increasing the concentration of these components in the reaction mixture, the SSH-*co*-MAA has a high percentage of gel (Fig. 9a). This is

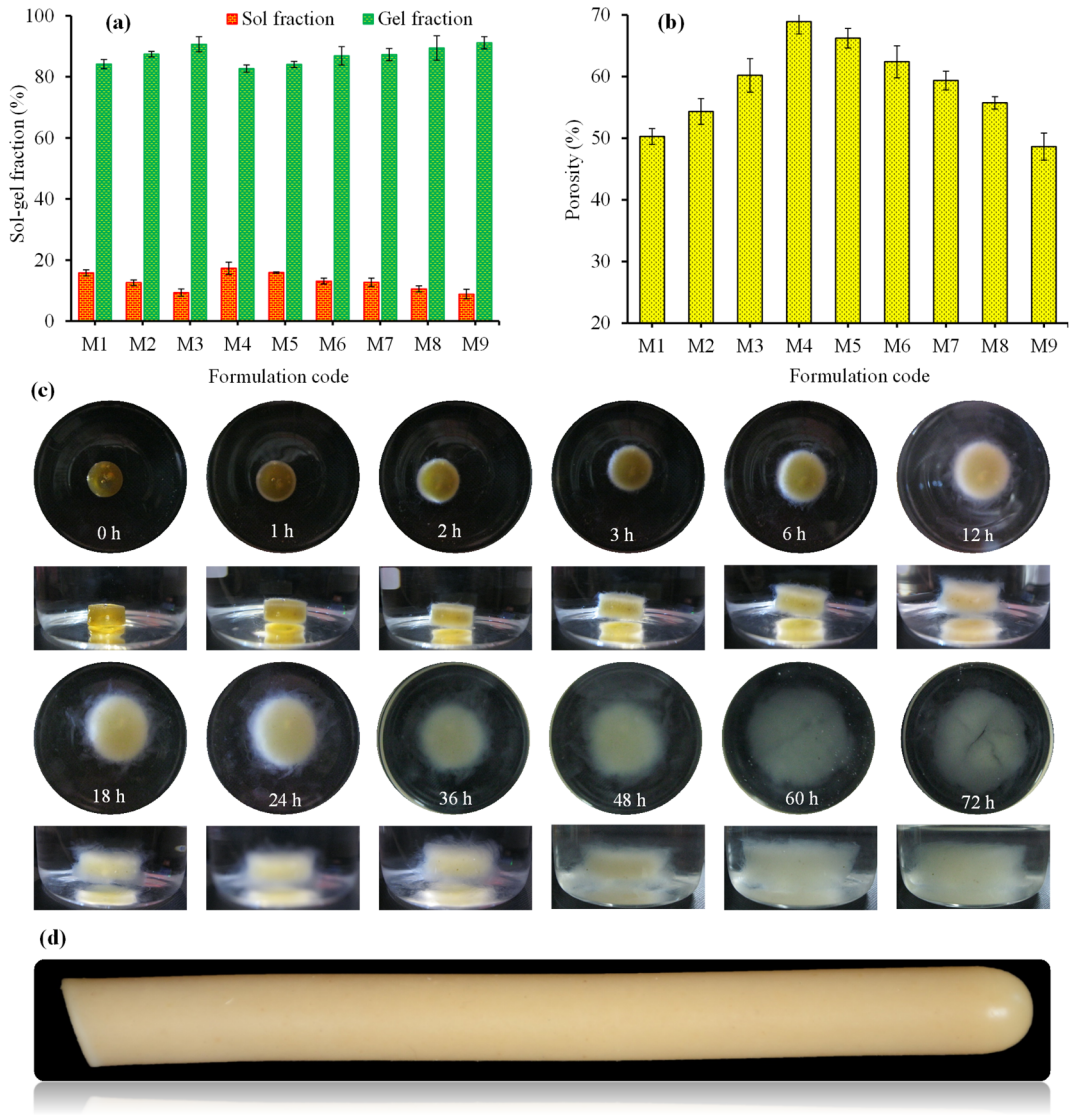

Fig. 9 Sol–gel fractions (%) (a) and porosity (%) (b) of SSH-*co*-MAA formulations, photographs of optimized formulation of SSH-*co*-MAA (M4) captured during swelling at pH 7.4 for 72 h (c), and photograph of M4 formulation captured after synthesis (d).

because the high concentration of SSH and MAA produced a greater number of free radicals in the reaction mixture and favor in rapid co-polymerization of SSH and MAA.[30] The increase in gel-fraction with the increase in the concentration of MBA was due to the formation of highly cross-linked SSH-*co*-MAA with high cross-linking density.[20] However, upon increasing the concentration of SSH, MAA, and MBA, the sol-fraction tends to decrease (Fig. 9a) which is due to the inverse relationship between gel-fraction and sol-fraction.[38]

3.5. Porosity measurement

Porosity measurement of any hydrogel system is used to study the influence of the concentration of polymer, monomer, and cross-linker on the size of the pores. In general, the larger the value of pore size of the hydrogel, the greater will be its water absorption potential of swelling media, and hence swelling increases. As a result, more drug will be loaded onto hydrogel and released from the hydrogel. Porosity measurement is considered an important characteristic of the hydrogel for its selection as sustained release DDSs.[29] Therefore, to evaluate the effect of SSH, MAA, and MBA on the pore size of the SSH-*co*-MAA, porosity was measured, and obtained results are presented in Fig. 9b. It was inferred that the percent porosity of SSH-*co*-MAA increased on increasing the concentration of SSH and decreased on increasing the concentration of MAA and MBA during the synthesis process. The increase in the concentration of SSH resulted in the increased number of OH groups in SSH-*co*-MAA due to which the hydrogen bonding became stronger. Consequently, the interconnected channels were produced and increased the porosity. However, by increasing the concentration of MAA and MBA, the porosity was decreased which may be due to the increase in the physical interaction between SSH and MAA, and the development of highly cross-linked material.[18]

3.6. Drug loading onto SSH-*co*-MAA

Venlafaxine HCl loading onto SSH-*co*-MAA was calculated through gravimetric and extraction methods and found the values in the range between 65.11 to 92.15 and 66.88 to 93.09 mg, respectively (Table 3).

A statistically non-significant difference between the amounts of venlafaxine HCl loading by both methods was found. A direct relationship between the amount of venlafaxine HCl loading onto SSH-*co*-MAA and its swelling indices was noted. Owing to high swelling, the cross-linking density and elasticity of polymeric structure decreased, hence the ability of SSH-*co*-MAA to capture the venlafaxine HCl increased. Whereas, due to lower swelling, both the cross-linking density and elasticity of polymeric structure increased resulting in decreasing the penetration ability of venlafaxine HCl to the SSH-*co*-MAA.[22] Moreover, the loading of venlafaxine HCl onto SSH-*co*-MAA was noted to be dependent on the concentration of SSH, MAA, and MBA in the formulation, *i.e.*, with the increase in the concentration of SSH, the amount of venlafaxine HCl loading was found to be increased. The same is true for MAA and MBA. The overall order of venlafaxine HCl loading was found to be M4 > M3 > M2 > M1 > M5 > M6 > M7 > M8 > M9.

3.7. *In vitro* drug release

The studies regarding *in vitro* venlafaxine HCl release from all formulations of VSSH-*co*-MAA were conducted in the buffers of pH 1.2, 4.5, 6.8, and 7.4 at 37 °C for 24 h. The obtained results are shown in Table 3 and Fig. 10. The venlafaxine HCl released from VSSH-*co*-MAA was found to be purely based on the swelling indices of SSH-*co*-MAA, pH of the dissolution media, and concentrations of the SSH, MAA, and MBA.[18] A negligible venlafaxine HCl release, *i.e.*, ≤9.67% was observed in the buffer of pH 1.2 after 24 h. However, upon changing the pH of the dissolution media to 4.5 (20.25%), 6.8 (74.76%), and 7.4 (89.11%), a significant amount of venlafaxine HCl release was noted after 24 h as mentioned in the parenthesis. The overall trend of cumulative venlafaxine HCl release (%) was observed as pH 1.2 < pH 4.5 < pH 6.8 < pH 7.4 (Table 3). It means that the maximum venlafaxine HCl was released at pH 7.4 for all formulations of VSSH-*co*-MAA because having maximum swelling of SSH-*co*-MAA at pH 7.4 and minimum release at pH 1.2 was due to negligible swelling of SSH-*co*-MAA at pH 1.2. Such pH-responsive drug release behavior could be beneficial for oral administration of different therapeutic agents, especially antibiotics, insulin, *etc.*, to release at intestinal pH after bypassing the stomach acidic environment.[39–41]

Table 3 Results of the loading of venlafaxine HCl onto SSH-*co*-MAA by gravimetric and extraction methods and venlafaxine HCl release in the buffer of pH 1.2, 4.5, 6.8, and 7.4

Formulation code	Drug loading (mg per disc)		Drug release (%) after 24 h			
	Gravimetric method	Extraction method	pH 1.2	pH 4.5	pH 6.8	pH 7.4
M1	81.89 ± 2.1	80.11 ± 1.6	6.11 ± 0.75	15.34 ± 0.84	51.77 ± 2.34	75.2 ± 3.31
M2	85.88 ± 1.77	83.90 ± 2.1	7.99 ± 0.61	17.55 ± 0.31	58.31 ± 1.14	79.7 ± 2.67
M3	89.9 ± 1.45	90.13 ± 1.76	8.67 ± 0.0.25	19.98 ± 0.57	67.23 ± 1.07	83.78 ± 1.99
M4	92.15 ± 2.3	93.09 ± 2.15	9.67 ± 0.0.17	20.25 ± 1.45	74.76 ± 3.56	89.11 ± 2.11
M5	80.12 ± 3.5	81.31 ± 2.18	5.88 ± 0.79	13.92 ± 1.01	49.78 ± 1.56	73.23 ± 2.45
M6	77.21 ± 1.1	76.89 ± 0.97	5.09 ± 0.13	12.51 ± 0.11	44.78 ± 2.08	68.69 ± 2.09
M7	72.17 ± 2.21	74.13 ± 2.3	4.99 ± 0.08	11.45 ± 0.98	43.11 ± 1.75	65.31 ± 2.17
M8	68.92 ± 3.1	67.56 ± 0.63	4.78 ± 0.10	9.75 ± 0.56	39.55 ± 1.15	62.09 ± 3.09
M9	65.11 ± 1.12	66.88 ± 2.33	4.65 ± 0.55	9.26 ± 0.78	35.54 ± 2.76	57.75 ± 2.15

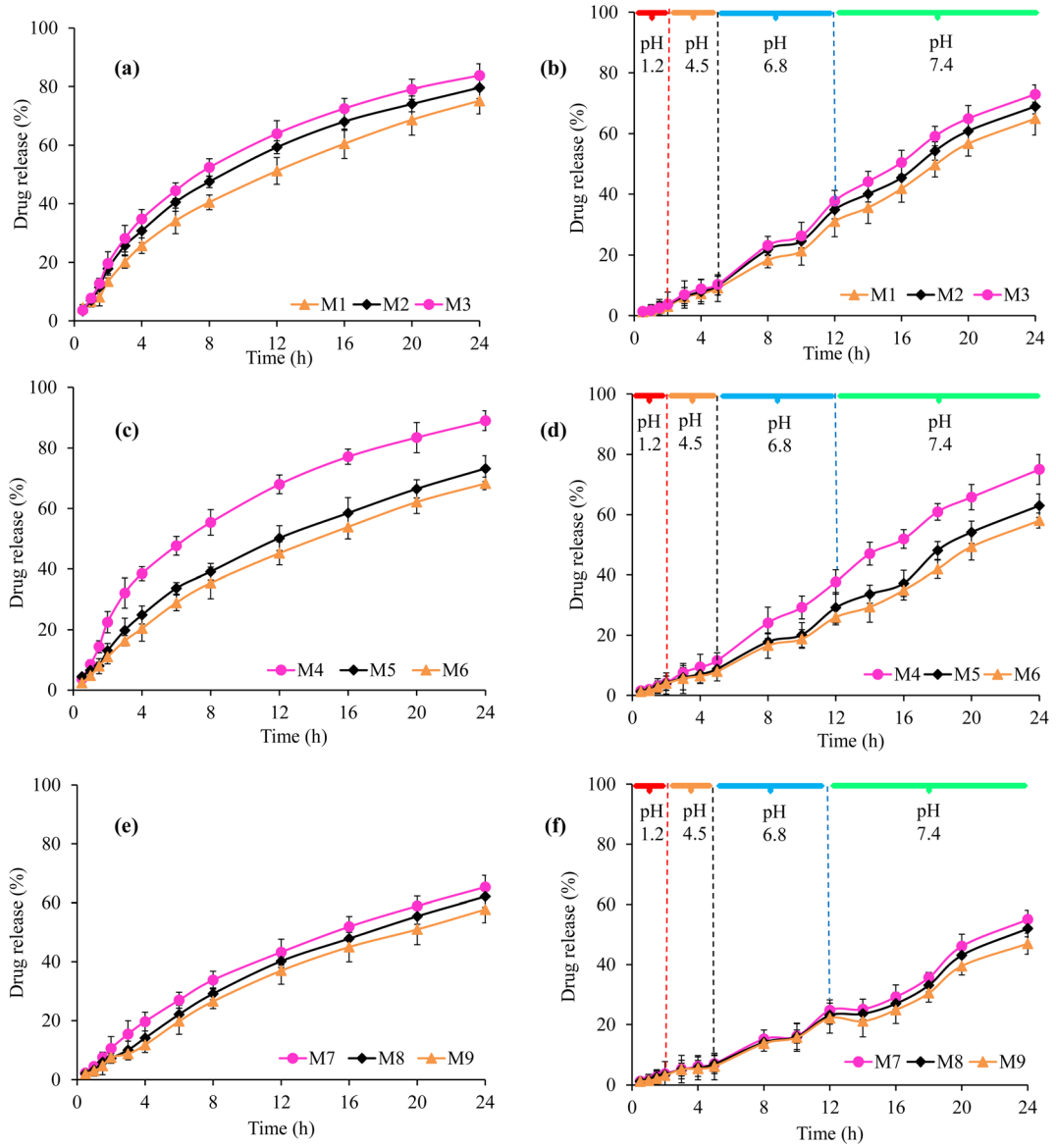

Fig. 10 *In vitro* release of venlafaxine HCl from VSSH-*co*-MAA at different concentrations of SSH (a) MAA (c) MBA (e) in the buffer of pH 7.4 and venlafaxine HCl release study performed at the pH and transit time mimicking the conditions of the GIT from VSSH-*co*-MAA at different concentration of SSH (b), MAA (d), and MBA (f).

Upon increasing the concentration of SSH from 1.5 to 2.5% the venlafaxine HCl released was found to increase from 6.11 to 8.67% at pH 1.2, 15.34 to 19.9% at pH 4.5, 51.77 to 67.23% at pH 6.8, and 75.2 to 83.7% at pH 7.4 after 24 h (Fig. 10a and Table 3). Such behavior is because the SSH is a stimuli-responsive swellable hydrophilic material and has been utilized in the development of intelligent DDSs. Due to the hydrophilic nature of SSH, its presence in the materials increased the swelling of hydrogels.[14] Therefore, upon increasing the concentration of SSH in the SSH-*co*-MAA the venlafaxine HCl release was found to increase from it.

Moreover, the release of venlafaxine HCl was found to decrease from 9.67 to 5.09% at pH 1.2, 20.25 to 12.51% at pH 4.5, 74.76 to 44.7% at pH 6.8, and 89.11 to 68.69% at pH 7.4 after 24 h once the concentration of MAA was increased from 30.0 to 37.5% (Fig. 10c and Table 3). The results showed that the venlafaxine HCl release behavior was consistent with the swelling indices. The formulation with the lowest concentration of MAA showed the maximum swelling. A possible explanation of this behavior might be that increasing the monomer concentration caused an increase in the cross-linking mass of the polymeric network and lead to the reduced flexibility of the polymeric chains. pH dependent drug release can be related to the restricted swelling of polymeric networks at low pH leading to limited diffusion of drug molecules whereas at high pH drug molecules were released at a faster rate owing to higher swelling ratios. Above behavior was due to the presence of hydrophilic groups and COOH group in MAA is responsible for its pH-sensitive behavior because COOH group of MAA ionizes at higher pH and employs repulsive forces in polymeric chains.[18]

Similarly, with the increase in the concentration of MBA from 0.6 to 1.0%, the venlafaxine HCl release was decreased from 4.99 to 4.65% at pH 1.2, 11.45 to 9.26% at pH 4.5, 43.11 to 35.54% at pH 6.8, and 65.31 to 57.75% at pH 7.4 (Fig. 10e and Table 3). By increasing the concentration of cross-linker over all swelling was reduced due to the growing cross-linking density of the polymer chain so venlafaxine HCl release was also decreased. It was evident that by escalating the MBA concentration, there was a decline in venlafaxine HCl release at all pH values owing to lessen in the mesh size of hydrogels, which hindered spreading out of the network and chain relaxation.

In GIT mimicking conditions, the results of *in vitro* venlafaxine HCl release from all formulations of VSSH-*co*-MAA are shown in Fig. 10. It was observed that at pH 1.2, the venlafaxine HCl release was 2.99% from formulation M1, 3.65% from formulation M2, and 3.78% from formulation M3 (Fig. 10b). Moreover, the release of venlafaxine HCl was found to increase up to 9.11, 9.88, and 10.34% at pH 4.5 (after 5 h), 31.0, 34.9, and 37.77% at pH 6.8 (after 12 h), and 65.0, 69.0, and 73.0% at pH 7.4 (after 24 h), respectively, from formulations M1, M2, and M3 (Fig. 10b). The results presented in the Fig. 10d indicated the effect of increasing concentration of MAA in the prepared hydrogel on drug release. It was observed that on increasing the concentration of MAA from 30.0 to 37.5%, the venlafaxine HCl release was decreased, *i.e.*, 4.10, 4.07, and 3.97% at pH 1.2 from formulation M4, M5, and M6, respectively after 2 h. Similarly, at pH 4.5, 11.55, 8.76, and 7.92% venlafaxine HCl was released after 5 h, at pH 6.8, the percentage of venlafaxine HCl released was noted as 37.67, 29.13, and 25.99% after 12 h, and at pH 7.4, the venlafaxine HCl release was observed as 75.02, 63.0, and 58.0% after 24 h from formulations M4, M5, and M6, respectively.

Moreover, with the increase in the concentration of MBA from 0.6 to 1.0%, the venlafaxine HCl release was found to be decreased due to a decrease in the swelling as shown in Fig. 5. Therefore, after 2 h, 3.71, 3.41, and 3.11% venlafaxine HCl was released from formulations M7, M8, and M9, respectively (Fig. 10f). However, after 5 h at pH 4.5, 7.0, 6.86, and 6.12%; after 12 h at pH 6.8, 24.80, 23.11, and 22.17%, and after 24 h at pH 7.4, 55.0, 52.0, and 47.0% venlafaxine HCl was released from formulation M7, M8, and M9, respectively.

Conclusively, the formulation M4 has shown a better swelling behavior as well as sustained drug releases profile as compared with other formulations.

3.8. Drug release kinetics and mechanism

The kinetics and mechanism of venlafaxine HCl release from VSSH-*co*-MAA were studied by fitting venlafaxine HCl release data to different kinetics models using DDSolver software. The results of kinetics data are presented in Table 4. The values of correlation coefficient (R^2) approaching "1" provided the best fit of the kinetic model to the release data. The value of n helps in determining the mechanism of venlafaxine HCl release. Based upon the value of R^2, the best fit model is first order indicating that the venlafaxine HCl release from a porous system is a concentration-dependent phenomenon. The value of n appears in the range from 0.553 to 0.817 determined through the Korsmeyer–Peppas model indicating that the venlafaxine HCl release followed the non-Fickian diffusion.[30,31]

SSH-*co*-MAA hydrogels are composed of polymeric backbones with ionic pendant groups (COOH group in MAA). In aqueous media of pertinent pH, the pendant groups ionize and produce fixed charges on the polymer network, creating electrostatic repulsive forces responsible for pH-dependent swelling thereby controlling the drug release. The existence of solvent in a glassy polymer causes the expansion of stresses that are lodged by an increase in the radius of gyration and end-to-end distance of polymer molecules, which is seen macroscopically as swelling. The movement of solvent molecules into the dry (glassy) polymer matrix takes place with a well-defined velocity front and a simultaneous increase in the thickness of the swollen (rubbery) region with time in the opposite direction.

Table 4 The kinetics data of venlafaxine HCl release from all formulations of VSSH-*co*-MAA in the buffer of pH 7.4

		Formulation code								
Release models		M1	M2	M3	M4	M5	M6	M7	M8	M9
Zero-order	R^2	0.8884	0.8120	0.7774	0.7504	0.8852	0.9229	0.9244	0.9681	0.9723
	K_0	3.647	4.031	4.308	4.582	3.544	3.257	3.109	2.869	2.652
	MSC	2.0259	1.5048	1.3357	1.2211	1.9980	2.3958	2.4161	3.2787	3.4183
First-order	R^2	0.9916	0.9850	0.9866	0.9881	0.9889	0.9945	0.9931	0.9984	0.9972
	K_1	0.062	0.077	0.089	0.102	0.059	0.051	0.047	0.041	0.037
	MSC	4.6078	4.0333	4.1483	4.2624	4.3365	5.0285	4.8142	6.2495	5.7110
Higuchi	R^2	0.9541	0.96048	0.8281	0.8560	0.7851	0.7559	0.7545	0.6900	0.6784
	K_H	14.469	16.203	6.999	8.064	6.031	5.465	5.213	4.675	4.300
	MSC	2.9156	3.1813	1.5944	1.7716	1.3707	1.2434	1.2376	1.0045	0.9679
Korsmeyer–Peppas	R^2	0.9907	0.9811	0.9890	0.9883	0.9957	0.9930	0.9931	0.9967	0.9962
	K_{KP}	9.731	12.753	14.430	16.049	9.548	7.708	7.313	5.097	4.473
	n	0.654	0.594	0.573	0.557	0.651	0.697	0.699	0.798	0.817
	MSC	4.3487	3.6350	3.3839	3.3372	4.3338	4.6282	4.6475	4.5689	4.4570
Hixson–Crowell	R^2	0.9743	0.9560	0.9559	0.9593	0.9701	0.9808	0.9801	0.9952	0.9944
	K_{HC}	0.018	0.021	0.024	0.028	0.017	0.015	0.014	0.012	0.011
	MSC	3.4945	2.9569	2.9547	3.0352	3.3442	3.8422	3.7502	5.1699	5.0252

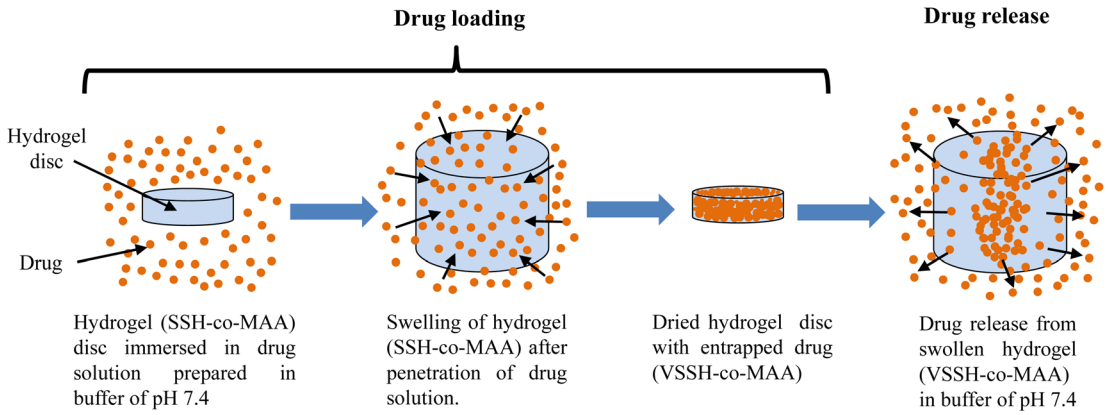

Fig. 11 Illustrated mechanism for the release of venlafaxine HCl from VSSH-*co*-MAA formulations.

Such swelling and diffusion do not generally follow a Fickian diffusion mechanism. The existence of a slow macromolecular relaxational process in the swollen region is believed to be responsible for the observed non-Fickian behavior both in swelling and drug release mechanism. Moreover, the high value of MSC for the first order model also supported the most appropriate model explaining the venlafaxine HCl release kinetics. The Fig. 11 is clearly evoked the mechanism of venlafaxine HCl release from VSSH-*co*-MAA formulations.

4. Conclusion

In this study, pH-sensitive hydrogel (SSH-*co*-MAA) based on mucilage from *S. spinosa* and MAA was synthesized through free radical copolymerization using different ratios of SSH, MAA, and the MBA. The structure, stability, and compatibility of the venlafaxine HCl with SSH-*co*-MAA were verified through the FTIR, solid-state CP/MAS ^{13}C NMR, PXRD, TGA-DSC, and SEM analyses. It was found that SSH-*co*-MAA is a supersorbent and thermally stable material. The swelling of properties of the SSH-*co*-MAA was pH-dependent as it offered higher swelling at pH 7.4, and lower swelling at pH 1.2. SSH-*co*-MAA showed pH-responsive swelling and de-swelling behavior. Furthermore, it was observed that the swelling behavior of SSH-*co*-MAA, drug loading onto SSH-*co*-MAA, and drug release from SSH-*co*-MAA were found to be increased by increasing the concentration of SSH and decreased by increasing the concentration of MAA and MBA. Sol–gel analysis indicated that gel-fraction has a direct relation with the concentration of SSH, MAA, and MBA. Porosity measurements revealed that the porosity has a direct relationship with the concentration of SSH and MAA and an inverse relationship with MBA. Hence, it can be concluded that SSH-*co*-MAA has the potential to sustain the release of drug for 24 h at the pH of small intestine. Due to inability of drug release from SSH-*co*-MAA at pH 1.2 make this novel drug delivery system an ideal candidate for site specific drug delivery and protection of the acid labile drug from degradation in harsh environment of stomach. Moreover, the stimuli-responsive swelling and deswelling behavior of SSH-*co*-MAA can be used for developing stimuli responsive drug delivery system. The highly porous nature of SSH-*co*-MAA can be exploited in tissue engineering, as a scaffold for bone regeneration and other biomedical applications, as well.

Author contributions

Arshad Ali: formal analysis, investigation, writing original draft, Muhammad T. Haseeb: review, editing, Muhammad A. Hussain: conceptualization, methodology, supervision, resources, Ume R. Tulain: validation, formal analysis, Gulzar Muhammad: formal analysis, validation, Irfan Azhar: investigation, resources, Syed Z. Hussain: data curation, investigation, Irshad Hussain: resources, validation, Naveed Ahmad: formal analysis.

Conflicts of interest

The authors declare that they have no conflicts of interest.

References

1 T. Miao, J. Wang, Y. Zeng, G. Liu and X. Chen, *Adv. Sci.*, 2018, **5**, 1700513.
2 Y. Sun, X. Jing, X. Ma, Y. Feng and H. Hu, *Int. J. Mol. Sci.*, 2020, **21**, 9151.
3 S. N. A. Bukhari, M. A. Hussain, M. T. Haseeb, A. Wahid, N. Ahmad, S. Z. Hussain, R. N. Paracha, M. U. Munir and M. A. Elsherif, *Gels*, 2022, **8**, 283.
4 J. Pushpamalar, A. K. Veeramachineni, C. Owh and X. J. Loh, *ChemPlusChem*, 2016, **81**, 504–514.
5 B. F. Far, M. R. Naimi-Jamal, M. Safaei, K. Zarei, M. Moradi and H. Y. Nezhad, *Polymers*, 2022, **14**, 5432.
6 F. Lin, J. Zheng, W. Guo, Z. Zhu, Z. Wang, B. Dong, C. Lin, B. Huang, B. Lu, B. Huang and B. Lu, *Cellulose*, 2019, **26**, 6861–6877.
7 A. Ali, M. A. Hussain, M. T. Haseeb, S. N. A. Bukhari, T. Tabassum and F. A. Sheikh, *J. Drug Delivery Sci. Technol.*, 2022, **69**, 103144.
8 A. Pourjavadi, R. Heydarpoura and Z. M. Tehrani, *New J. Chem.*, 2021, **45**, 15705–15717.

9 P. Sikdar, M. Mazbah Uddin, T. M. Dip, S. Islam, M. S. Hoque, A. K. Dhare and S. Wu, *Mater. Adv.*, 2021, **2**, 4532–4573.
10 A. S. Volokhova, K. J. Edgar and J. B. Matson, *Mater. Chem. Front.*, 2020, **4**, 99–112.
11 M. M. Al-Gharaibeh, H. R. Hamasha, S. Lachmuth and I. Hensen, *Plant Species Biol.*, 2017, **32**, 25–35.
12 A. Danin, *Bocconea*, 1992, **3**, 18–42.
13 M. B. Bahadori, H. Valizadeh, B. Asghari, L. Dinparast, M. M. Farimani and S. Bahadori, *J. Funct. Foods*, 2015, **18**, 727–736.
14 K. M. Nadkarni, *The Indian Materia Medica. Chopra's "I.D. of I"*, 1996, vol. 1, p. 593.
15 A. Ali, M. A. Hussain, A. Abbas, T. A. Khan, G. Muhammad, M. T. Haseeb and I. Azhar, *Cellul. Chem. Technol.*, 2022, **239**, 239–250.
16 A. Ali, M. A. Hussain, M. T. Haseeb, M. U. Ashraf, M. Farid-ul-Haq, T. Tabassum, G. Muhammad and A. Abbas, *J. Braz. Chem. Soc.*, 2023, 1–13.
17 M. Aslam, K. Barkat, N. S. Malik, M. S. Alqahtani, I. Anjum, I. Khalid, U. R. Tulain, N. Gohar, H. Zafar and A. C. Paiva-Santos, *Pharmaceutics*, 2022, **14**, 1218.
18 F. Shabir, A. Erum, U. R. Tulain, M. A. Hussain, M. Ahmad and F. Akhter, *Des. Monomers Polym.*, 2017, **20**, 485–495.
19 M. Chen, Z. Ni, Y. Shen, G. Xiang and L. Xu, *Colloids Surf., A*, 2020, **602**, 125133.
20 H. Gao, K. Min and K. Matyjaszewski, *Macromolecules*, 2007, **40**, 7763–7770.
21 N. Gull, S. M. Khan, O. M. Butt, A. Islam, A. Shah, S. Jabeen, S. U. Khan, A. Khan, R. U. Khan and M. T. Z. Butt, *Int. J. Biol. Macromol.*, 2020, **162**, 175–187.
22 S. Nisar, A. H. Pandit, M. Nadeem, A. H. Pandit, M. M. A. Rizvi and S. Rattan, *Int. J. Biol. Macromol.*, 2021, **182**, 37–50.
23 M. Gibaldi and S. Feldman, *J. Pharm. Sci.*, 1967, **56**, 1238–1242.
24 A. W. Hixson and J. H. Crowell, *Ind. Eng. Chem.*, 1931, **23**, 1160–1168.
25 T. Higuchi, *J. Pharm. Sci.*, 1963, **52**, 1145–1149.
26 R. W. Korsmeyer, R. Gurny, E. Doelker, P. Buri and N. A. Peppas, *Int. J. Pharm.*, 1983, **15**, 25–35.
27 P. I. Ritger and N. A. Peppas, *J. Controlled Release*, 1987, **5**, 37–42.
28 M. S. Iqbal, J. Akbar, M. A. Hussain, S. Saghir and M. Sher, *Carbohydr. Polym.*, 2011, **83**, 1218–1225.
29 S. Ganguly, S. Mondal, P. Das, P. Bhawal, P. P. Maity, S. Ghosh, S. Dhara and N. C. Das, *Int. J. Biol. Macromol.*, 2018, **111**, 983–998.
30 J. A. Torres-Ávalos, L. R. Cajero-Zul, M. Vázquez-Lepe, F. A. López-Dellamary, A. Martínez-Richa, K. A. Barrera-Rivera, F. López-Serrano and S. M. Nuño-Donlucas, *Polymers*, 2021, **13**, 533.
31 A. Olad, M. Pourkhiyabi, H. Gharekhani and F. Doustdar, *Carbohydr. Polym.*, 2018, **190**, 295–306.
32 L. S. Bernardi, P. R. Oliveira, F. S. Murakami, M. A. S. Silva, S. H. M. Borgmann and S. G. Cardoso, *J. Therm. Anal. Calorim.*, 2009, **97**, 729.
33 A. Ali, M. A. Hussain, M. T. Haseeb, U. R. Tulain, M. Farid-ul-Haq, T. Tabassum, G. Muhammad, S. Z. Hussain, I. Hussain and A. Erum, *React. Funct. Polym.*, 2023, **182**, 105466.
34 N. R. Singha, M. Mahapatra, M. Karmakar, A. Dutta, H. Mondal and P. K. Chattopadhyay, *Polym. Chem.*, 2017, **8**, 6750–6777.
35 S. A. Shah, M. Sohail, M. U. Minhas, N. Rehman, S. Khan, Z. Hussain, Mudassir, A. Mahmood, M. Kousar and A. Mahmood, *Drug Delivery Transl. Res.*, 2019, **9**, 555–577.
36 H. Schott, *J. Pharm. Sci.*, 1992, **81**, 467–470.
37 S. Huang, J. Wang and Q. Shang, *J. Biomater. Sci., Polym. Ed.*, 2017, **28**, 194–206.
38 S. A. Dergunov, I. K. Nam, G. A. Mun, Z. S. Nurkeeva and E. M. Shaikhutdinov, *Radiat. Phys. Chem.*, 2005, **72**, 619–623.
39 T. Su, W. Zhao, L. Wu, W. Dong and X. Qi, *Int. J. Biol. Macromol.*, 2020, **163**, 366–374.
40 X. Qi, Y. Yuan, J. Zhang, J. W. M. Bulte and W. Dong, *J. Agric. Food Chem.*, 2018, **66**, 10479–10489.
41 X. Qi, W. Wei, J. Li, T. Su, X. Pan, G. Zuo, J. Zhang and W. Dong, *Mater. Sci. Eng., C*, 2017, **75**, 487–494.